AIAA JOURNAL
Vol. 42, No. 3, March 2004

Generation of Three-Dimensional Turbulent Inlet Conditions for Large-Eddy Simulation

P. Druault*
Université Pierre-et-Marie-Curie, 78210 Saint Cyr l'Ecole, France
S. Lardeau†
Imperial College of Science, Technology, and Medicine, London, England SW7 2BY, United Kingdom
and
J.-P. Bonnet,‡ F. Coiffet,§ J. Delville,¶ E. Lamballais,** J. F. Largeau,§ and L. Perret§
Université de Poitiers, 86962 Futuroscope Chasseneuil CEDEX, France

A method for generating realistic (i.e., reproducing in space and time the large-scale coherence of the flows) inflow conditions based on two-point statistics and stochastic estimation is presented. The method is based on proper orthogonal decomposition and linear stochastic estimation. This method allows a realistic representation with a minimum of information to be stored. Most of the illustrations of this method are given for a plane turbulent mixing layer that contains most of the basic features of organized turbulent flows. Examples of the application of the method are given first for the generation of inflow conditions for direct numerical simulation (DNS) and for large-eddy simulation from experimental results. Second, DNS results are used to generate realistic inflow conditions for two- and three-dimensional DNS, retaining only a minimum size of relevant information.

Introduction

Importance of Coherent Structures

THE existence of coherent or organized motions has been recognized for at least the past three decades. Although there is no definitive consensus on the definition of coherent structures (CS), an organized character, at large scales (of the order of the characteristic gradient zones) of most turbulent flows, is generally observed, mainly from visualizations. However, as far as turbulent flows are concerned, such CS are embedded inside a randomly distributed field, and their identification and characterization are not straightforward. This identification has to be done for several purposes: first, for a simple energetic point of view because CS can represent, after Fiedler,[1] from 10% (for boundary layers and far jets) up to 20% (far wakes, plane mixing layers) or 25% (near wakes or jets) of the total kinetic energy; and second, because the dynamical properties of CS play an essential role in mixing processes, drag, noise emission, etc. The energy content of CS is not the only characteristic that has to be addressed. Their redistributive capabilities are also of crucial importance. The impact on flow measurement and on data-processing techniques is obvious. Simple, one-point statistics are not sufficient for a correct characterization of most turbulent flows. In addition, the choice of a predictive approach has to be made according to the organized character of the flow.

Coherent Structures and Their Modeling

The large-eddy simulation (LES)[2] is one of the methods for predicting flows in which large-scale structures play an important role. It is one of the most popular techniques both for academic and practical applications.

Other approaches have been proposed in a pioneering way by Ha Minh[3,4]: the semideterministic method (SDM) followed by the so-called unsteady Reynolds-averaged Navier–Stokes (URANS).[5] LES and SDM/URANS approaches are similar in a sense that both involve a filtering process: a low-pass filtering (LES) or a more global filtering approach (SDM). LES takes into account the unresolved scales (at the level of the computational mesh) through a specific closure, relating these small scales to the resolved quantities. LES involves a low-pass filter, in a conventional Fourier decomposition sense. SDM/URANS postulates that the turbulent field can be decomposed in term of a coherent (deterministic) part, directly related to the flow configuration, on which a random (more universal) part is superimposed. In this case, the applied filter does not simply correspond to a low-pass filter as in LES. The filter used by SDM can be considered as a structure filter. Following this approach, the unfiltered part is resolved by schemes comparable to direct numerical simulation (DNS). Additional universal transport equations have to be used for the random part—the coherent and random fields being coupled by a specific closure. More recently, Farge and Schneider[6] have proposed a new simulation approach [coherent vortex simulation (CVS)] based also on the representation of turbulent flows in two parts: one part considered as being out of equilibrium, and the other being considered as thermalized motion.

In some sense, SDM and CVS are both based on a structure filter; the SDM uses the CS as the major definition (the random part being the rest of the field) when CVS considers that the random field is the thermalized part, the CS part being considered as the rest of the field.

Need for Realistic Inflow Conditions

The specification of realistic inflow boundary conditions for all of these numerical methods is a central question. Adrian et al.[7] present the state of the art of the problems linked to the determination of the turbulent inflow characterization methods. For a spatially

Presented as Paper 2003-0065 at the AIAA 41st Aerospace Sciences Meeting, Reno, NV, 6–9 January 2003; received 17 July 2003; revision received 10 October 2003; accepted for publication 23 October 2003. Copyright © 2003 by the American Institute of Aeronautics and Astronautics, Inc. All rights reserved. Copies of this paper may be made for personal or internal use, on condition that the copier pay the $10.00 per-copy fee to the Copyright Clearance Center, Inc., 222 Rosewood Drive, Danvers, MA 01923; include the code 0001-1452/04 $10.00 in correspondence with the CCC.

*Assistant Professor, Laboratoire de Mécanique Physique, Unité Mixte de Recherche 7068, Centre National de la Recherche Scientifique.
†Research Associate, Department of Aeronautics.
‡Research Director, Laboratoire d'Etudes Aérodynamiques, Unité Mixte de Recherche 6609, Centre National de la Recherche Scientifique, École Nationale Supérieur de Mécanique et Aérotechnique. Member AIAA.
§Ph.D. Student, Laboratoire d'Études Aérodynamiques, Unité Mixte de Recherche 6609, Centre National de la Recherche Scientifique, École Nationale Supérieur de Mécanique et Aérotechnique.
¶Research Engineer, Laboratoire d'Etudes Aérodynamiques, Unité Mixte de Recherche 6609, Centre National de la Recherche Scientifique, École Nationale Supérieur de Mécanique et Aérotechnique.
**Assistant Professor, Unité Mixte de Recherche 6609, Centre National de la Recherche Scientifique, École Nationale Supérieur de Mécanique et Aérotechnique.

developing flow, the most common method is to impose small perturbations on a laminar mean flow profile at the inflow section of the computational domain and to compute the transition of the flow. This method requires the use of a very long streamwise domain in order to allow the full development of turbulence. If only the turbulent state of the flow is under study, the need to compute the complete transition is clearly a drawback because of the high computational cost of such DNS/LES.

For a fully turbulent situation, turbulent mean velocity profiles can be used and some more or less random noise superimposed in order to start some artificial perturbation supposed to mimic the real instantaneous behavior of the turbulent flow. In this case, the code has to build a pseudoturbulent development downstream of the inflow conditions for convective flows for example. This development region has no physical significance in general and is of no practical interest. Nowadays, as far as we know, no simulation code exists that directly uses highly turbulent conditions as inlet conditions.

These aspects obviously also prevent applications such as flow control. In this case, the inflow conditions should vary in time, and then some computations of controlled flows can be impossible.

Another important feature of practical importance that cannot be taken into account by simulations is the role of rare events. For practical applications, such as aeronautics or industrial processes, some exceptional events can be observed, such as large-amplitude and short-duration excitation whose immediate effect on the flow can be dramatic. Numerical simulations can be very detailed in space, can be very precise in temporal resolution, but are (because of their cost) limited by the time sample length they can describe. Therefore, the probability that these rare events are naturally captured is very low. Then, any procedure that allows for prescribing especially these events (from a specific sequence of experimental data for example) and their effects on CS can be useful.

Inlet Conditions: State of the Art

Usually, the generation of the inflow boundary condition consists of using random velocity fluctuations superimposed on the mean velocity profile. But even if a sophisticated boundary data-generation method preserving the spectral and spatial distributions of the fluctuations is used,[8–11] the lack of realistic turbulent structures induces a transient region near the inlet. The synthetic character of inflow data prevents the velocity derivatives from quickly achieving a nonzero skewness, leading to an inhibition of the nonlinear transfers near the inlet. A solution can consist of using an auxiliary (temporal or spatial) simulation where velocity data are stored at a given section corresponding to the inlet boundary of the main simulation.[12–15] Such a technique provides satisfactory results for specific studies, but its application remains difficult for complex flow configurations. Moreover, such calculations are expensive in time and/or storage capacities. The specification of realistic inflow conditions remains still open. For the last development of inflow conditions generation for LES, the reader can refer to Sagaut[16] and references therein.

The strategy proposed here consists of the generation of inflow conditions using time-varying experimental data. This methodology detailed in the next section is based on the use of experimental time histories arising from hot-wire probes. From these measurements obtained at a few selected reference locations, the instantaneous velocity field is reconstructed (interpolated and extrapolated) at a given set of grid points corresponding to the inlet mesh of a numerical simulation. Then this reconstructed velocity field is used as an inflow condition for a numerical code permitting the simulation of the downstream development of the experimental flow. In this context, the measurement section for the experiment, or the inflow section for the DNS/LES, can be viewed as a real/virtual interface. This concept is schematically illustrated in Fig. 1 for the typical case of a spatially developing mixing layer considered hereafter. It should be emphasized that such an experiment/simulation association can be considered as a procedure for generating realistic inflow conditions for a numerical simulation, but also as a procedure for a dynamical data postprocessing, where the DNS/LES is used to improve experimental data by restoring the part of the information that has been missed or deteriorated during the measurement step.

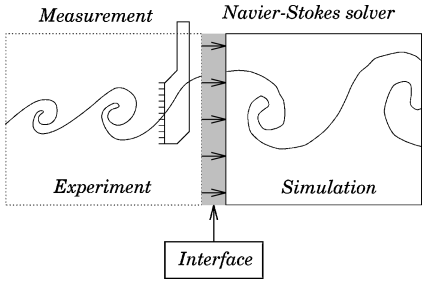

Fig. 1 Schematic representation of an experiment/simulation interface for a spatially developing mixing layer.

Details on these approaches and concepts can be found in Druault et al.[17] and in Lamballais and Bonnet.[18] In a comparable study, Maruyama et al.[19] propose to take into account the coherence of the flow in the immediate vicinity of a few measurement points in order to built realistic inflow data for LES. The present approach proposes a more global analysis, based on a description of the entire flow domain. The approach of Maruyama et al. is perhaps better adapted to a specific flow but can be difficult to generalize.

Strategy for Realistic Space–Time Reconstruction

Principles

To separate the CS from incoherent turbulence, we make use of the multiple decomposition. For a given streamwise section x_0 normal to the mean flow, this decomposition can be written as

$$u_i(x_0, y, z, t) = \overline{U_i}(x_0, y, z) + \tilde{u_i}(x_0, y, z, t)$$

with

$$\tilde{u_i}(x_0, y, z, t) = \hat{u_i}(x_0, y, z, t) + u_i'(x_0, y, z, t) \qquad (1)$$

where $\overline{U_i}$ is the (conventional) time average and $\hat{u_i}$ and u_i' are, respectively, the coherent and incoherent fluctuations. For sake of simplicity, x_0 will be omitted in the rest of the text.

To generate realistic inflow conditions, let us examine each term of the decomposition. $\overline{U_i}$ being stationary, it is prescribed from the mean velocity profiles. $\overline{U_i}$ can be obtained simply from analytical, experimental, or computational results. In the present approach, the coherent part, $\hat{u_i}(y, z, t)$, is estimated from the knowledge of the large-scale structures of the flow. As far as experiments are considered, it is always difficult to extract the organized character of the flow and also to estimate the corresponding coherent signals on a finer mesh.

To obtain spatiotemporal information from experiments, two major methods are usually available: quantitative visualizations (PIV-HPIV) or simultaneous measurements by distributed sensors (for example, hot-wires rakes). The first solution provides a quite satisfactory spatial resolution, but the associated temporal resolution is still insufficient for an accurate description of the nonstationary character of many flow configurations. Conversely, the high-frequency bandwidth of the second method provides a satisfactory representation of the temporal evolution of the flow. In this second case, however, simultaneous measurements of the three velocity components are only possible at a limited number of points. Thus, with such an experimental arrangement only a limited knowledge of the spatial organization of the flow is available. Consequently, the development of an optimal interpolation/extrapolation procedure permitting the estimation, from a small number of velocity measurements, of a complete velocity field at each numerical grid point located at the inflow boundary of the computational domain for sake of data storage reduction is required.

To summarize, the proposed interface concept needs to address the following three steps:

1) Step one requires instantaneous velocity measurements by a limited number of probes or references points. The location of these probes has to be optimized in order to gain maximum significant instantaneous information about the spatial organization of the flow (related to the CS description of the flow).

2) Step two is the reconstruction of velocity data in the measurement section at a given set of grid points, via interpolation/extrapolation procedures preserving the coherent character of the flow.

3) Step three is the simulation of the downstream development of the flow, using the resulting reconstructed velocity data as inflow conditions.

The basic idea of the method is to use the linear stochastic estimation (LSE) as a data-processing tool able to estimate the large-scale behavior of the velocity in an inflow section, from the knowledge of the two-point correlation coefficients and of time histories obtained at a limited number of locations in this reference plane. This reconstructed part of the velocity signal can be considered as the coherent part of the signal, that is, $\hat{u}_i(y, z, t)$. The use of a complete sets of time histories allows for a good representation of the quasi-deterministic character of the CS but also allows us to take into account the possible rare events.

However, the use of LSE can suffer from some practical problem, linked to the nonuniformity of the estimation into the domain. Then, we introduce the proper orthogonal decomposition as a complementary tool. These two methods are described in the next sections.

In addition to this essential part of the inflow condition, the last, random part of the signal should be introduced: $u_i'(y, z, t)$. For that purpose, a minimum level of randomness has to be introduced through a given amount of noncorrelated, random noise.

Proper Orthogonal Decomposition

A very useful decomposition can be introduced in order to address this interface problem: proper orthogonal decomposition (POD, introduced by Lumley[20]) or its generalization, biorthogonal decomposition (introduced by Aubry et al.[21]). In this approach, the signal is projected onto intrinsic modes of the flow. These modes are representative of energetic events. They are determined from the two-point correlation tensor by solving an eigenvalue problem. Symbolically the instantaneous contribution of the POD modes can be written as

$$\tilde{u}(X, t) = \sum_n a_n(t)\Phi^{(n)}(X)$$

where $X = (x, y, z)$ is the spatial coordinate and $a_n(t)$ is obtained by projecting the flow realization $\tilde{u}(X, t)$ onto the POD eigenvectors $\Phi^{(n)}(X)$:

$$a_n(t) = \int_{\mathcal{D}} \tilde{u}(X, t)\Phi^{(n)}(X)\,\mathrm{d}X \tag{2}$$

where $\Phi^{(n)}$ is the solution of the eigenvalue problem:

$$\int_{\mathcal{D}} \overline{\tilde{u}(X, t)\tilde{u}(X', t)}\Phi^{(n)}(X')\,\mathrm{d}X' = \lambda^{(n)}\Phi^{(n)}(X)$$

This method can be applied to turbulent data coming either from hot-wire rakes [in this case the conventional proper orthogonal decomposition (POD) is used] or from snapshot results [from particle image velocimetry (PIV) for example]. In this last case, the snapshot POD is used.[22]

In the case of plane turbulent mixing layers, experimental results have been obtained from two rakes of 12 X–wire probes lying in the (y, z) plane (i.e., normal to the mean convection velocity; see Delville et al.[23]). Druault[24] computed the coherent and random spectra that can be defined by truncating the series to the first four POD modes (Fig. 2). The first modes clearly extract the typical frequency peak associated to the Kelvin–Helmoltz two-dimensional instability. The rest of the signal (corresponding to the remaining modes) exhibits a spectrum corresponding to a quasi-homogeneous (equilibrium) turbulence. This characteristic shows that the CS detected from POD are not localized in the spectral domain. They correspond to multiple scales and differ from usual Fourier filtering in time or space approaches: in some sense these POD modes lead to a decomposition very close to the one used in URANS or SDM computational methods.

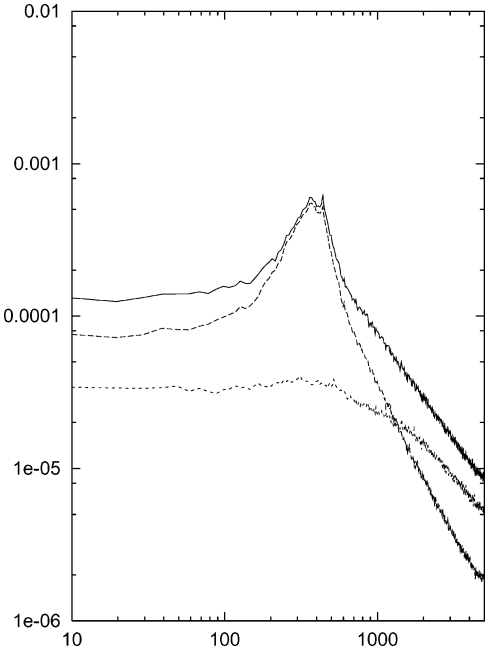

Fig. 2 CS extraction via POD in a plane turbulent mixing layer.[24] Plotted are, vs frequency (Hz), ——, the directly measured v spectrum (original); - - - -, the contribution of first four POD modes to this spectrum (coherent); and · · · ·, the spectrum of the remaining modes (incoherent).

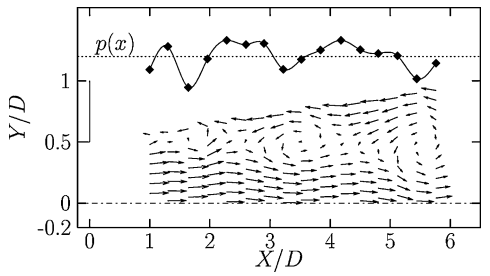

Fig. 3 CS eduction from LSE. Estimated velocity vector field induced by the instantaneous axial-pressure distribution in the near field of a round jet[26]: 16 microphones + X hot-wire probes.

Linear Stochastic Estimation

In the LSE, introduced by Adrian,[25] some reference signals are considered as conditioning the rest of the signals. In this approach, one tries to linearly estimate $\hat{u}(X, t)$, the conditioned flowfield from the knowledge of N_r references signals $p_r(t)$. This estimation is performed through the knowledge of the two-point correlation tensor. Symbolically, the LSE can be written as

$$\hat{u}^{est}(X, t) = \sum_{r=1}^{N_r} a_r(X)p_r(t)$$

where $a_r(X)$ is the solution of the following equations:

$$\overline{\tilde{u}(X, t)\,p_q(t)} = \sum_{r=1}^{N_r} a_r(X)\overline{p_r(t)p_q(t)}, \qquad q = 1, \cdot, N_r$$

u and p_r can be chosen as any flow characteristic (velocity, temperature, pressure, etc.). An illustration of this method is given in Fig. 3. In the experiment of Picard and Delville,[26] a rake of 16 pressure transducers is placed in the vicinity of a turbulent jet, and a rake of X hot wires is displaced in the shear zone of the jet mixing layer. From the pressure–velocity correlations, LSE allows then the estimation of the instantaneous velocity field associated with the instantaneous longitudinal pressure distribution.

Such a method is very useful for simple estimation of instantaneous field, this estimation being considered as a conditional one.

The important difference with conventional conditional method is that LSE does not require any thresholding or adaptation procedure. The only parameter to be chosen is the location and nature of the reference signal(s). Another advantage is the possibility of association with other methods, particularly with the POD through the complementary method.

Complementary Method

The complementary LSE+POD approach consists of projecting the velocity field estimated from LSE procedure onto the POD eigenfunctions to access to the instantaneous POD projection coefficients $a_n(t)$ (Ref. 27). This method is particularly useful when the space–time correlation tensor is known and when instantaneous signals are known in a very few number of points.[28,29]

Spatial Correlation Tensor Modeling

The two-point spatial correlation tensor of velocity contains a large amount of information about the large-scale structures of turbulent flows. Particularly, eddy structure identification methods such as POD or LSE are based on this tensor. Applying these identification methods can require the knowledge of the correlation tensor over the whole turbulent flow domain. This information requiring expensive capabilities is only available from numerical methods. Conversely, when dealing with experimental data the correlation tensor is only available at a few selected locations. This section presents methods for interpolating and extrapolating a two-point correlation tensor known only at a few discrete nodes. These methods lead to gain a continuous description of this tensor on any finer and broader mesh.

1) To perform an interpolation of spatial correlation tensor $R_{ij}(y, y') = \widetilde{u_i}(y)\widetilde{u_j}(y')$, a convenient Gram–Charlier expansion based on Hermite polynomials can be used.[30] We approximate this tensor by superimposing N_{GC} Gram–Charlier expansions such as each polynomial corresponds to a spatial-scale contribution. Then we can estimate $R_{ij}(y, y')$ as

$$\widetilde{R}_{ij}(y, y') = \sum_{k=1}^{N_{GC}} P_k \exp(-Qk)$$

where polynomials P_k and Q_k are expressed with equations:

$$P_k = P_{00}^k + P_{20}^k\left(y - y_0^k\right)^2 + P_{11}^k\left(y - y_0^k\right)\left(y' - y_1^k\right) + P_{02}^k\left(y' - y_1^k\right)^2 + \ldots \quad (3)$$

$$Q_k = Q_{20}^k\left(y - y_0^k\right)^2 + Q_{11}^k\left(y - y_0^k\right)\left(y' - y_1^k\right) + Q_{02}^k\left(y' - y_1^k\right)^2 \quad (4)$$

The unknown coefficients are solved through a least-mean-square procedure. This interpolation method provides a continuous description of the spatial correlation tensor within the measurement domain, which can be used for POD or LSE approaches as well.

2) The Gram–Charlier procedure can also be used for extrapolation of the correlations. However, because the polynomial part dominates the exponential part for large separations $|y - y'|$ this procedure is not well suited for extrapolation. Extrapolation is needed for large separation because the experimental determination of the correlation is difficult because of the vanishing value of turbulent activity in these regions.

POD can be used as a complementary tool for this extrapolation. With the POD, the cross-correlation tensor $R_{ij}(y, y')$ can be expressed in term of the POD eigenvalues and eigenvectors in the following way:

$$R_{ij}(y, y') = \sum_{n=1}^{N} \lambda^{(n)} \Phi_i^{(n)}(y) \Phi_j^{(n)}(y') \quad (5)$$

The extrapolation procedure consists therefore of extrapolating individually each POD eigenvector. By construction, each POD mode follows individually the flow properties,[31] and then it is possible to perform a realistic extrapolation for large spatial separation. For example if the turbulence level vanishes at infinity or near a boundary, each POD mode behaves in the same way. The extrapolation of the correlation tensor corresponds in this context to the much more simple extrapolation of the POD modes. This extrapolation can be performed by considering that each POD eigenfunction vanishes exponentially.

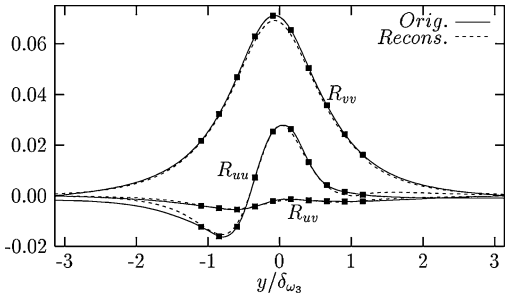

Fig. 4 Two-point correlation tensor interpolated and extrapolated from 10 reference points superimposed on the exact ones (data arising from a two-dimensional simulation of a plane mixing layer,[32] reference points located on the mixing-layer axis).

Finally a Schmidt procedure is needed to ensure the orthonormality of the extrapolated eigenvectors before the correlation tensor can be rebuilt by using Eq. (5). This procedure has been validated[32] by using numerical data stemming from a two-dimensional simulation of a plane mixing layer (described in the next section). An illustration is given in Fig. 4 where the entire two-point correlation tensor is reconstructed from only 10 reference points.

Example of Local Velocity Field Reconstruction

In this section, the potential of the reconstruction technique for generating velocity data at a given streamwise self-similar section x_0 is illustrated by using numerical or experimental data. In this case, because the turbulent intensity is on the order of 10% at the inlet, the computation has difficulties absorbing such a high level of perturbation. Consequently, the inlet section is followed by a short transient adaptation region.

To illustrate the possibilities offered by an experiment/simulation interface, we will consider in the rest of the paper the case of a spatially developing mixing layer between two streams of velocities U_1 and U_2, with $U_1 > U_2$ and $\Delta U = U_1 - U_2$, in a Cartesian frame of reference $(Oxyz)$, where x, y, z are, respectively, the streamwise (mean flow), transverse (normal to the splitter plate), and spanwise directions. In this frame, (u, v, w) or (u_1, u_2, u_3) are the velocity components.

Numerical Data LSE Reconstruction

To test the efficiency of the proposed reconstruction method, the case of numerical data is now considered.[33] The velocity data are stored at each time step in a given section $x = x_0$ during a two-dimensional simulation of a spatially evolving mixing layer (for information about the flow configuration, see the section on numerical interface testing for two-dimensional DNS). To mimic a typical experimental situation, these datas are stored at only three grid points. The two velocity components are then estimated using LSE for each grid point. The quality of this reconstruction is illustrated in Fig. 5, where a temporal sequence of the reconstructed vorticity is compared with the "exact" one. Note that for these vorticity data, a Taylor's hypothesis is used for the calculation of streamwise derivatives. Comparison between exact and reconstructed vorticities shows that the large-scale structures of the flow are well reproduced, whereas fine-scale details of vorticity are quite deteriorated, especially in the filaments regions. Despite this reservation, it is worth noting that the information about velocity data at only three points allows the representation of the large-scale organization of the flow with the correct phase information concerning the large-scale vortices.

Experimental Data Reconstruction

We considered a spatially developing mixing layer with a velocity ratio of 0.44. For the example shown here, the interface (i.e., the measurement section) is located in the self-similar region of the flow

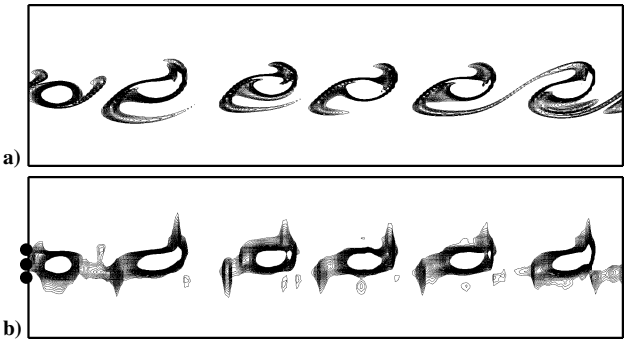

Fig. 5 Temporal sequences of instantaneous spanwise vorticity at $x = x_0$ $[\omega_z = -(1/U_c)(\partial v/\partial t) - (\partial u/\partial y)$ using Taylor's hypothesis with the convection velocity $U_c = (U_1 + U_2)/2]$: a) exact reference one and b) reconstructed one with LSE procedure from three y-reference locations. The locations of the reference points (●) are given on the figure (vertical, transverse y direction; and horizontal, time arbitrary units).

where the mixing layer reaches a fully turbulent state.[24] This configuration corresponds to the schematic view presented on Fig. 1. The experimental data are velocity measurements performed in a section normal to the streamwise direction. A two-dimensional hot-wire rake composed of 33 X-probes is used in order to obtain simultaneous measurements. Each probe provides the u component, whereas v and w are obtained alternatively on a staggered rectangular grid of 3×11 positions equally distributed in transverse y and spanwise z directions, respectively. The measurement domain extends over $\delta_{\omega_0} \times 3.33\delta_{\omega_0}$, δ_{ω_0} being the local vorticity thickness. These data are used to build a temporal sequence of velocity data. Starting from velocity measurements at these few locations, an approximation of velocity data is performed on the inlet section of the computational domain, by means of interpolation/extrapolation procedures:

1) In a first step, the statistical homogeneous spanwise z direction is processed. In this specific direction, periodic condition required by numerical simulation must be imposed on the experimental data that obviously are not periodic. A POD approach is then performed from experimental data. In this spanwise direction, each POD eigenvector is close to harmonic mode. This property comes from the homogeneous character of the flow providing POD degenerates into Fourier modes for homogeneous situation.[34] One of the advantages of using a POD approach to this spanwise direction is that eigenvectors have wave length that are not directly related to the size of domain on which POD is applied. The eigenvectors $\Phi^{(n)}$ are then analytically modeled through sinusoidal data and afterward extrapolated to cover the minimal size Λ_z of periodic dimension larger than the rake extent (Fig. 6a).

2) In a second step, a method based on LSE is applied to rebuild velocity data in the normal y direction.

3) Finally, velocity are scaled using experimental normal Reynolds stresses $\widetilde{u_i^2}(y)$. Such a procedure leads to an underestimation of about 50% of $\widetilde{\tilde{u}\tilde{v}}$.

The advantage of using such experimental data as inflow condition is the possibility to introduce the spatiotemporal coherence of the mixing layer. Figure 6b (Ref. 35) shows vertical velocity isosurfaces of the reconstructed data in a convected frame of reference using Taylor's hypothesis in the temporal direction. Realistic behavior of the flow motion can be observed with the preservation of large-scale spanwise structures exhibiting roughly a $3\delta_{\omega_0}$ streamwise spacing with a realistic three-dimensional character.

Numerical Testing of Inflow Conditions

In the following we present several numerical computations : a DNS approach, a LES highly resolved in space, and a LES with a more industrial-like spatial resolution. The first two codes are developed in the LEA laboratory. The last one corresponding to a lower computational cost, using a code named PEGASE, has been developed at ONERA. These different numerical simulations have been used 1) to analyze the significant criteria to be checked to ensure realistic inflow conditions and 2) to test reconstructed experimental velocity as inflow condition.

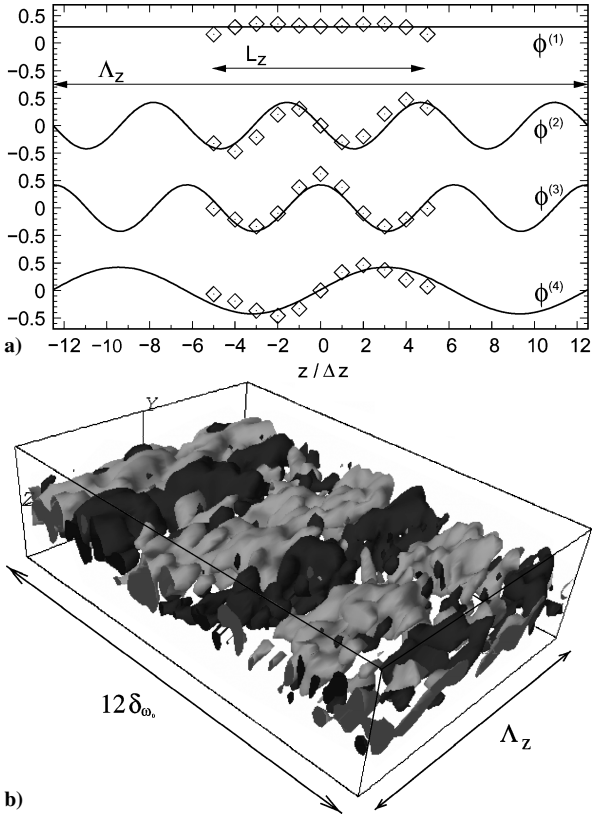

Fig. 6 Example of the first four eigenvectors on the spanwise measurement domain L_z (◇) and their models on the periodic domain Λ_z (——): a) velocity component v in the middle of the mixing layer (top), and b) isosurfaces of vertical reconstructed velocity $\tilde{v} = \pm 0.1$ (from Coiffet et al.[35]). Data are normalized using the inflow vorticity thickness δ_{ω_0} and the velocity difference $U_1 - U_2$.

We first used DNS as a tool for the determination of selected criteria permitting to ensure realistic inflow conditions.

Numerical/Numerical Interface Testing for Two-Dimensional DNS

Numerical Method

A two-dimensional spatially developing plane mixing layer with a velocity ratio of 0.44 is considered by Druault et al.[33] The Reynolds number based on the initial vorticity thickness δ_{ω_i} and ΔU is $Re = 200$. The numerical code incompact3D[36] used here solves the incompressible Navier–Stokes equations on a regular and nonstaggered Cartesian grid $(n_x, n_y) = (1001, 201)$ corresponding to a domain size of $(L_x, L_y) = (280\delta_{\omega_i}, 56\delta_{\omega_i})$. Sixth-order compact centered differences schemes are used to evaluate all spatial derivatives,[37] except near the in- and outflow boundaries where single-sided schemes are employed for the streamwise derivative calculation. Equations are integrated in time using a third-order Adams–Bashforth scheme. Free-slip boundary conditions are applied at $y = \pm L_y/2$, whereas outflow boundary conditions at $x = L_x$ are determined through the resolution of a simplified convective equation.

Results

A first calculation is performed in a large computational domain (extent in the streamwise direction $L_x = 280\delta_{\omega_i}$). During this reference calculation, at a streamwise location (x_0; see Fig. 7 top) where the flow is physically realistic, the velocity components are stored for each point on the full virtual interface. Using only a part of this information, several set of inflow conditions are tested to perform secondary simulations where the computational domain is truncated upstream from the virtual interface. The principle of this procedure can be easily understood by examining Fig. 7, where different inflow conditions are compared for a spatial mixing layer. The

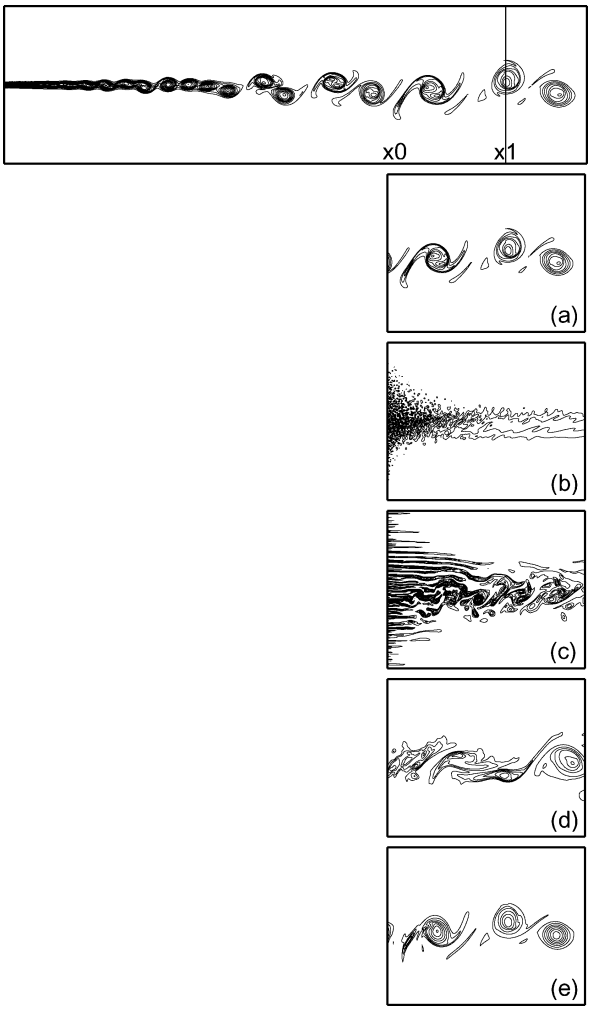

Fig. 7 Spanwise vorticity contours: top, reference simulation ($L_x = 280\delta_{\omega_i}$), a–e, truncated simulations ($L'_x = 100\delta_{\omega_i}$) using inflow conditions detailed in the text.

advantage of this purely numerical method is that it is possible, by comparison to the reference simulation, to evaluate accurately the benefit (or the lack of benefit) obtained when inflow data are matching a given statistical property. In the work of Druault et al.,[17] the well-known strong sensitivity of the mixing layer to inlet conditions (already observed for both experimental and numerical configurations) is clearly confirmed. When the complete knowledge of the flow variables is used to specify the inflow conditions (all velocity components at each grid point on the inlet plane), a quasi-perfect agreement was found (Fig. 7a) because of the strong convective character of the mixing layer for which the downstream development of the flow has a negligible effect on the upstream conditions. The second kind of inflow conditions considered by Druault et al.[17] (Fig. 7b) corresponds to random velocity fluctuations spatially and temporally uncorrelated (white noise) but constrained to reproduce the energy of each component of the Reynolds-stress tensor. This inflow generation technique, quite easy to perform, has clearly a dramatic effect on the realism of the simulation, in qualitative (lack of turbulent structure) and quantitative (considerable fall of kinetic energy near the inlet, Fig. 8b) terms. Two intermediate cases were also considered by Druault et al.,[17] who tested inflow conditions preserving temporal (Fig. 7c) and spatial (Fig. 7d) two-point correlations. The improvement obtained from these inflow data emphasized the importance of the correct representation of the temporal and spatial spectra. However, because of the lack of realistic spatial coherence corresponding to the turbulent structures in these synthetic inflow conditions, a transient downstream of the inlet can be clearly observed. A more efficient method for generating more realistic inflow conditions using a time history of velocity data at a small number

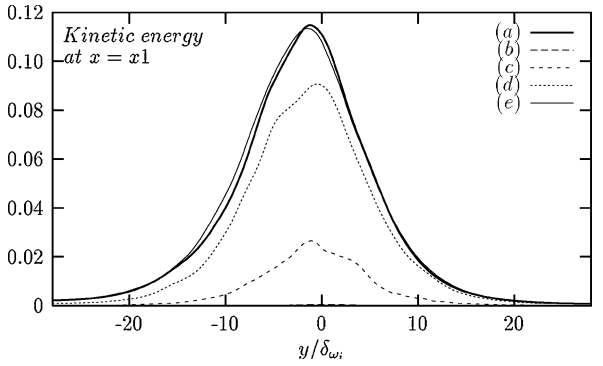

Fig. 8 Fluctuating kinetic energy at $x = x_1$ obtained from previous truncated DNS simulations a), b), c), d), and e).

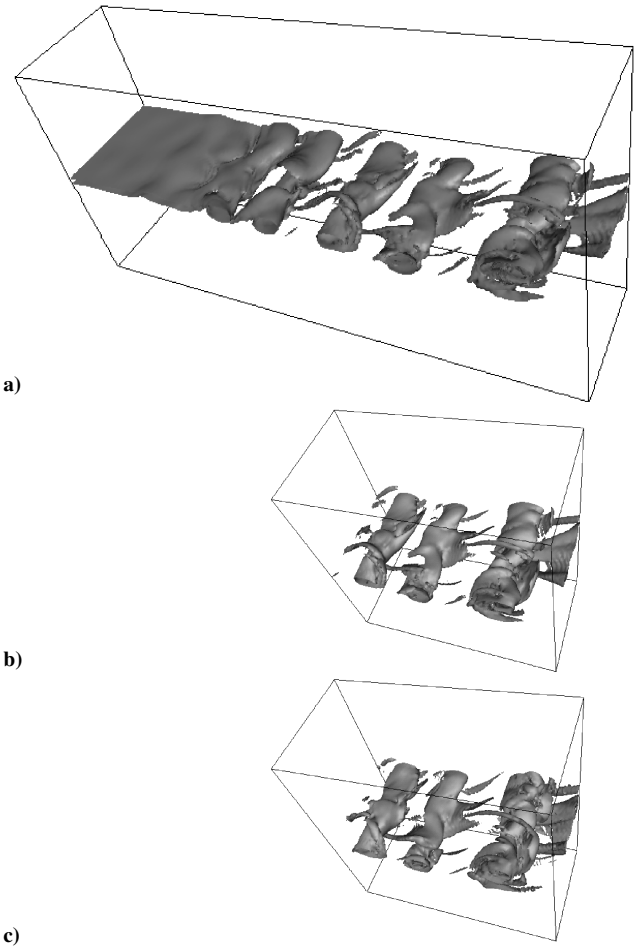

Fig. 9 Spanwise vorticity surface: a) Reference simulation ($L_x = 100\ \delta_{\omega_i}$); b) truncated simulations ($L'_x = 50\delta_{\omega_i}$) using exact inflow conditions; and c) velocity field reconstructed with LSE procedure from the knowledge of stored data at three y points in each z location.

of points was just described. Druault et al.[17] choose to use velocity data stored at only three points. The inflow conditions obtained by the method described in the preceding section reduce efficiently the transient near the inlet (Fig. 7e). As far as the energy is concerned, Fig. 8 shows clearly the efficiency of the method.

The main conclusion of this study is that for the inlet data generation the spatiotemporal coherence of the inflow must be necessary for preserving the organized character of the turbulent motion at large scale. The same procedure has been used for a three-dimensional DNS.[24] Figure 9 illustrates the efficiency of the method that requires only 3% of the entire data for a satisfactory computation.

Experimental/Numerical Interface Testing for Low-Resolution LES

A first attempt to generate inflow conditions from experimental data was done by using results arising from mixing-layer experiments with a velocity ratio of 0.59. Times histories of the streamwise and the transverse velocity components (u, v) are obtained from a rake of 12 equally spaced X-wires in a self-similar section. The Reynolds number based on the local vorticity thickness δ_{ω_0} is equal to 9×10^4. The experimental instantaneous velocity field is then reconstructed at each node of the inlet computational grid of the numerical code using LSE procedure.[38]

Numerical Method

A description of the numerical method including the mixed scale model used can be found in Sagaut et al.[39] Briefly, the computational domain is equal to $20\delta_{\omega_0} \times 10\delta_{\omega_0} \times 7\delta_{\omega_0}$, and a nonuniform Cartesian grid including $(151 \times 71 \times 36)$ points is used.[38] The nondimensional time step is equal to 2×10^{-3}, which is equivalent to a physical data-acquisition frequency of 750 kHz (75 times the sampling frequency of the experiment). A linear interpolation in time is used in order to generate the velocities at the required time steps.

A periodic boundary condition is used in the spanwise direction. In the transverse direction, a simplified representation of the solid walls is achieved using a no-slip condition. A zero-stress-like condition is used at the outflow, coupled to a buffer zone to prevent spurious reflections.

The estimation of inflow condition is based on a LSE of the large-scale structures according to the method presented in the preceding section. The level of the random noise superimposed is adjusted in such a way that the fluctuations of kinetic energy have the same energy in their coherent and incoherent part. The realistic turbulent inflow conditions presented here have to be considered as a demonstrator of the method. It is indeed clear that several combinations of coherent/random parts have to be tested. It was not the purpose of this preliminary study to give a definitive answer of the best ideal solution but to illustrate on a given example the possibilities of the method.

In the spanwise direction, the coherent field is homogeneous, and the large-scale structures "entering" the flow that are generating are nominally two-dimensional: the reconstructed experimental velocity field is duplicated at each spanwise location. The w component is here purely random, with a spectral behavior corresponding to the experimental observations.

Results

With the LSE-based inflow condition, despite the poor resolution of the computation, the flow corresponds to a real turbulent flow from its beginning. The spreading of the flow is clear on the snapshot visualization of the vorticity modulus (Fig. 10). This point will be discussed quantitatively later. The computed development of the initially quasi-two-dimensional structures is complex and

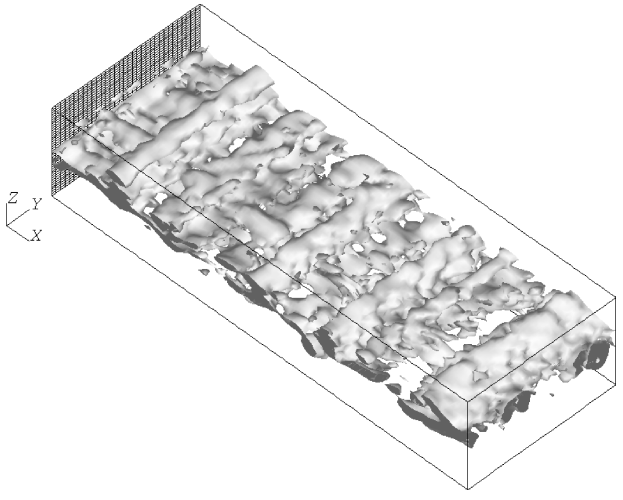

Fig. 10 Instantaneous vorticity modulus.

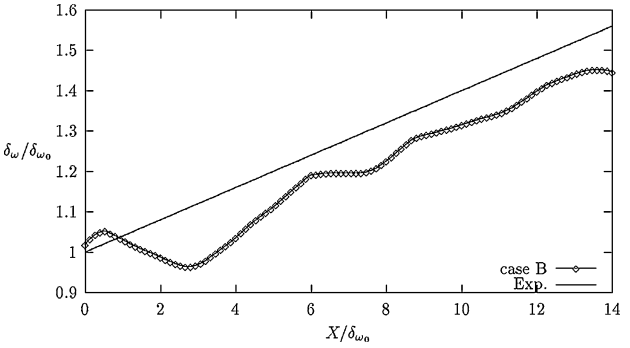

Fig. 11a Vorticity thickness.

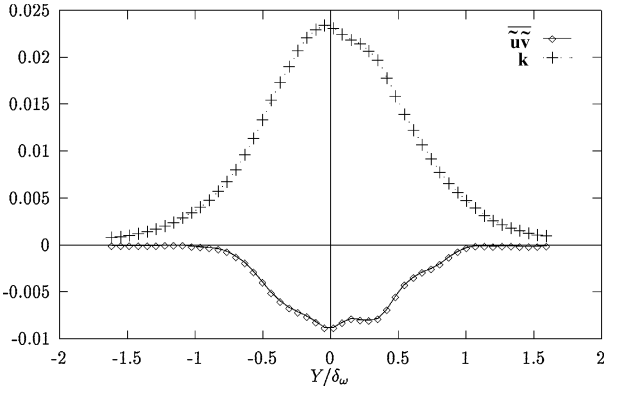

Fig. 11b Shear stress and kinetic energy normalized with ΔU^2.

closely corresponds to the different processes occurring in mixing layers. Pairings processes are observed. Streamwise vortices ("braid"), known to play essential role in the dynamics of mixing layers, are also observed. These structures were not introduced at the inflow conditions. Then, it is clear that the present method is quite efficient as far as complex three-dimensional structures of the flow are relevant. A more quantitative analysis is given next.

Figure 11a shows the evolution of the vorticity thickness δ_ω. For comparison, the conventional evolution of δ_ω is provided. The evolution of the computed δ_ω closely agrees with the expected one, except for some irregularities, because of simulation data.

It is also clear from Fig. 11a that the simulation shows very rapidly downstream of the inflow plane the expected mixing-layer development. As far as the turbulent fields are concerned, Fig. 11b shows the shear stress and kinetic turbulent energy.

The mean and turbulent distributions correspond to the conventional ones for turbulent plane mixing layers, with maxima of shear stress in close agreement with the measured values, that is, typically $10^{-2}\Delta U^2$ ($\Delta U = 17$ m/s). In addition, the ratio $\widetilde{u}\widetilde{v}/k$ is below 0.3, a value generally accepted for turbulent mixing layer.

However, from the present computation,[38] a detailed analysis of the turbulent Reynolds stresses shows that the ratio $\widetilde{w}^2/\widetilde{v}^2$ is underestimated compared to the experimental results.

This preliminary study showed certain limitations caused by the non-three-dimensional character of experimental inflow conditions. In this sense, a new experimental arrangement (a two-dimensional rake of 33 X wires just detailed) has been developed permitting to access to the instantaneous three-dimensional CS. With such equipment, a new experimental database has been obtained in a self-similar streamwise section of the plane mixing layer with a velocity ratio of 0.44. Some other tests are performed with a high-resolution LES using reconstructed three-dimensional experimental data as inflow condition.

Experimental/Numerical Interface Testing for High-Resolution LES

Numerical Method

LES of a spatially developing mixing layer is performed using the structure function model developed by Lesieur and

Métais.[2] The incompressible Navier–Stokes equations are solved on a regular and nonstaggered grid. The domain dimensions are $(L_x, L_y, L_z) = (18.3\delta_{\omega_0}, 8\delta_{\omega_0}, 8.33\delta_{\omega_0})$ corresponding to a grid of $(n_x, n_y, n_z) = (193, 97, 96)$. The same numerical code Incompact3D just described is used with the same set of boundary conditions. The Reynolds numbers based on the local vorticity thickness δ_{ω_0} and ΔU of the experiment and the inlet of the LES are identical ($Re = 6.6225 \times 10^4$).

Experimental turbulent inflow conditions are generated at the inlet. The procedure for reconstructing the experimental instantaneous velocity fields has been detailed in the preceding section. Recall that these experimental data are obtained from a two-dimensional rake of 33 X-wires probes corresponding to 66 velocity components measurements. Based on these 66 times histories, we reconstruct the three velocity components at each grid node of the inlet section corresponding to $(97 \times 96 \times 3 = 27936)$ velocity components.

Results

The results presented here should be considered as preliminary ones. In particular the issue of the sensitivity to the grid resolution and the domain extent has not been examined. These studies being important for further developments, they will be investigated in the near future.

Figure 12a shows a vorticity visualization, obtained by the computation presented here. A fast regeneration of large-scale spanwise structures seems to occur—this tendency being more easily identified by vertical velocity visualization (Fig. 12b). Longitudinal vortices can also be clearly observed on vorticity visualization.

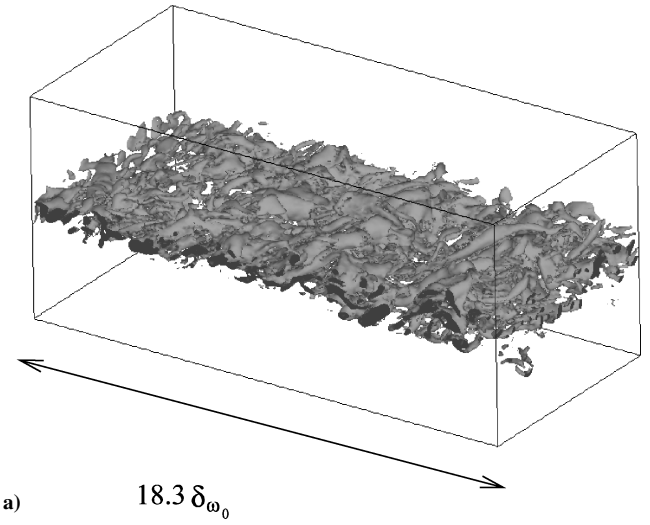

Fig. 12 Isosurfaces of a) vorticity modulus $\omega = 1.8$ and b) vertical velocity $\tilde{v} = \pm 0.08\Delta U$ (from Coiffet et al.[35]). Results of a LES using turbulent experimental data as inflow conditions.

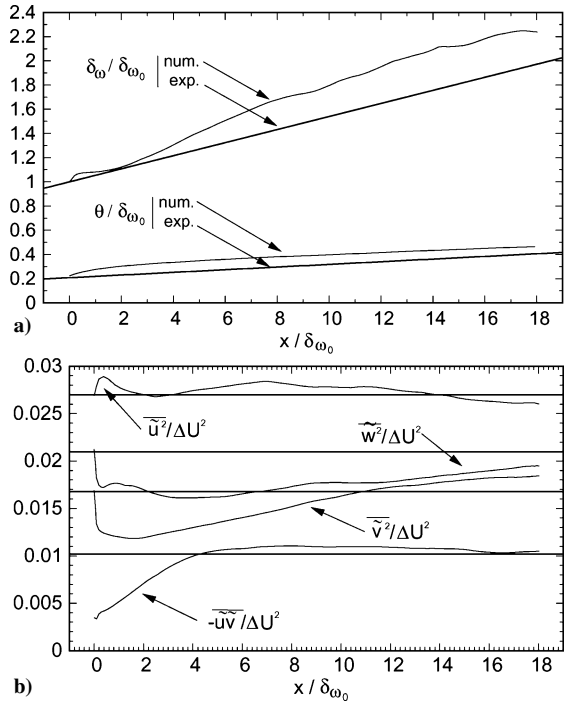

Fig. 13 Streamwise evolution of the vorticity thickness δ_ω, the momentum thickness θ, and the Reynolds-stress maxima max $\overline{\tilde{u}_i\tilde{u}_j}$. LES using reconstructed experimental data as inflow conditions.[35]

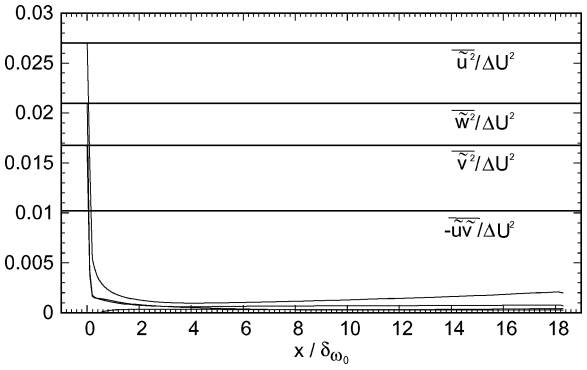

Fig. 14 Streamwise evolution of the Reynolds-stress maxima max $\overline{\tilde{u}_i\tilde{u}_j}$: white-noise data (from Coiffet et al.[35]).

The streamwise evolution of different characteristic quantities of the flow is presented in Fig. 13. As far as the thicknesses are concerned, the correct growth rate is recovered although a zone of extra-amplification (3 δ_{ω_0} long) appears. This effect can be interpreted by observing the Fig. 13b. Indeed, because of the normalization method of the reconstructed experimental fluctuating part (see Experimental Data Reconstruction Section), which forces the incoherent part of the fluctuations to zero, the shear stress $\overline{\tilde{u}\tilde{v}}$ has been underestimated. As a consequence, the correlation level between the longitudinal and the transversal fluctuations is far from its natural value. It appears that the region necessary to recover the correct growth rate corresponds roughly to the zone required to retrieve the correct equilibrium between the turbulent components. For the same reasons, the other quantities $\tilde{u}_i^2$ deteriorate in the beginning of the computational domain and only recover asymptotically their inflow value.

A solution to overcome this drawback is to keep a realistic ratio between the coherent and noncoherent parts [see Eq. (1)]. Such a process is currently under study. Moreover, because of the experimental

procedure the cross components are estimated on a coarser mesh (twice) than the u-component one. It can be anticipated that the smallest scales are then less accurately estimated for v and w than for u, which can lead to a deterioration of the shear stress. Considering these drawbacks, no attempt has been made in the present study to analyze in details the resulting spectral and spatial coherence. However, a visual analysis of the Fig. 12 suggests that the spatial as well as the temporal (via a Taylor hypothesis) behavior corresponds to the expected large-scale characteristics of such a flow. More quantitative studies are under development.

The advantage of using coherent experimental data can be estimated by comparison with an equivalent LES using time and space uncorrelated inflow data (white noise preserving only the Reynolds stresses). Everything being equal, a second computation with these inflow conditions is made, and mean results are plotted in Fig. 14. A dramatic breakdown of all of the Reynolds stresses is observed, and the computation becomes totally unrealistic (Fig. 14).

Conclusions

The determination of inflow conditions for direct numerical simulation (DNS) and large-eddy simulation (LES) is a crucial issue, particularly for practical applications of computations of spatially evolving turbulent flows. In this paper, we recall some basic features about the large-scale structures, which, in general, dominate the dynamics of turbulent shear flows. The need for correct spatiotemporal estimation of inflow conditions leads to consider in particular the spatial coherence of the flows while storing a minimum amount of information. Then, the data processing based on two-point statistics [such as proper orthogonal decomposition (POD), linear stochastic estimation (LSE), and combined methods] is a natural approach. Such a methodology has been tested on experimental LES interfaces. For sake of optimization, a DNS/DNS validation approach has also been used. It then appears that 1) to generate realistic inflow condition, it is much more efficient to preserve the spatio temporal coherence of inflow data rather than the spatial and spectral one-point energy distributions; and 2) the use of the reconstruction method based on LSE seems to be efficient for inflow condition generation with a good compromise between data compression and three-dimensional rendering.

During the DNS tests, we focus on plane mixing layers, and, based on our earlier experimental experience, we consider three reference points in the mean shear direction. The optimal choice of the number and the location of these reference points (and stored data) is not straightforward if the flow is not known a priori in term of its spatial organization. A research program is under development with the TAM of Urbana–Champaign (Illinois) in order to derive some optimal procedure based on a description of the flow in term of the POD modes. This procedure will have the advantage of an objective approach.

As far as a statistically homogeneous direction (for plane or axisymmetric configurations) is concerned, the problem can be more complex, and the reduction of the number of reference points is still an open problem. The combined method proposed here can be a solution, but the transversal, three-dimensional character of the CS has to be taken into account.

From experiments, we apply the method to the measurements obtained with a rake of hot wires. We run two kinds of LES, with different levels of resolution. Even with a poorly resolved computation presenting some drawbacks with conventional inflow conditions, the present method allows for a spectacular improvement. A quantitative study in the case of a better resolved LES shows that further studies should be necessary. In particular, the spanwise characteristics have to be addressed in more details, and the part of random signal has also to be adjusted.

For practical applications, other difficulties can appear. The first one can be encountered for wall-bounded flows where several scales have to be taken into account, depending of the distance from the wall. In this case, zonal analysis can be used. A second class of flows that can be difficult to handle with this method is the compressible one. In this case, the choice of the relevant reference variable(s) is not straightforward. Moreover, experiments for this kind of flow are much more difficult. The combination of numerical simulations and limited experimental data can be a possible way to overcome these limitations.

As far as experiments are used to provide the necessary information, the use of rakes of sensors as presented here is not always possible. Other experimental procedures can advantageously be developed. As an example, the spatial correlation needing POD and LSE can be obtained through PIV or HPIV in a plane for two-dimensional slices, or with two PIV slices. The correlation tensor can be obtained only from statistical averages, and then no temporal sequences are needed at that stage. Temporal signals for building the complete set of inflow conditions can separately be obtained by a limited number of simultaneous time-resolved histories. Such signals can be obtained for example from a limited number of hot wires or microphones. The proposed method can then take advantage of the combination of the good spatial resolution but no time evolution of PIV with the poor spatial resolution with good temporal response of hot-wire anemometry.

Some other roads are also open with regard to the generation of spatial correlations and time histories. For simple flows, stability analysis can provide some information about the typical spatial and temporal relevant scales. Then, with simple models the spatial correlations can be estimated, avoiding any experiment resolved in space. In addition, the same stability analysis can provide a temporal evolution that can be used as an initial template. Lastly, research under progress is devoted to dynamical systems identification or POD Galerkin projection that can provide realistic time evolutions. Finally, let us emphasize that these new possible approaches for generating "synthetic turbulence" are promising tools not only for experimental/LES interfaces, but also for hybrid Reynolds-averaged Navier–Stokes/LES methodologies.

Acknowledgments

The study presented in this paper has been performed with the support of the French ministry of Defense (P. Moschetti), of ONERA (P. Sagaut), and of IDRIS (CNRS) computing center. We are also grateful to H. Garem for his contribution to experimental design.

References

[1]Fiedler, H. E., "Control of Free Turbulent Shear Flows," *Flow Control: Fundamental and Practices*, edited by M. Gad-el-Hak, A. Pollard, and J. P. Bonnet, Springer, Heidelberg, Germany, 1998, pp. 336–429.

[2]Lesieur, M., and Métais, O., "New Trends in Large Eddy Simulations of Turbulence," *Annual Review of Fluid Mechanics*, Vol. 28, 1996, pp. 45–82.

[3]Ha Minh, H., "Order and Disorder in Turbulent Flows: Their Impact on Turbulence Modelling," Osbourn Reynolds Centenary Symposium, UMIST, Manchester, England, U.K., May 1994, Paper 8.

[4]Ha Minh, H., "La Modélisation Statistique de la Turbulence: Ses Capacités et ses Limitations," *Compte Rendu de l'Académie des Sciences, Série IIb*, Vol. 327, No. 4, 1999, pp. 343–358.

[5]Hanjalic, K., and Kenjeres, S., "Simulation of Coherent Eddy Structure in Buoyancy-Driven Flows with Single-Point Turbulence Closure Models," *Closure Strategies for Turbulent and Transitional Flows*, edited by B. Launder and N. Sandham, Cambridge Univ. Press, Cambridge, England, U.K., 2001, pp. 659–684.

[6]Farge, M., and Schneider, K., "Coherent Vortex Simulation (CVS), A Semi-Deterministic Turbulence Model Using Wavelets," *Flow, Turbulence and Combustion*, Vol. 66, No. 4, 2001, pp. 393–426.

[7]Adrian, R. J., Meneveau, C., Moser, R. D., and Riley, J. J., "Final Report on 'Turbulence Measurements for LES' Workshop," Univ. of Illinois, TAM Rept. 937, UILU-ENG-2000-6012, Urbana, IL, 2000.

[8]Lee, S., Lele, S. K., and Moin, P., "Simulation of Spatially Evolving Turbulence and the Applicability of Taylor's Hypothesis in Compressible Flow," *Physics of Fluids*, Vol. 4, No. 7, 1992, pp. 1521–1530.

[9]Le, H., and Moin, P., "Direct Numerical Simulation of Turbulent Flow over a Backward-Facing Step," Dept. of Mechanical Engineering, Stanford Univ., CTR Rept. TF 58, Stanford, CA, Dec. 1994.

[10]Le, H., Moin, P., and Kim, J., "Direct Numerical Simulation of Turbulent Flow over a Backward-Facing Step," *Journal of Fluid Mechanics*, Vol. 330, 1997, pp. 349–374.

[11]Lesieur, M., Begou, P., Briand, E., Danet, A., Delcayre, F., and Aider, J. L., "Coherent-Vortex Dynamics in Large-Eddy Simulation of Turbulence," *Journal of Turbulence*, Vol. 4-016, 2003, pp. 1–24.

[12]Akselvoll, K., and Moin, P., "Large Eddy Simulation of Turbulent Confined Coannular Jets," *Journal of Fluid Mechanics*, Vol. 315, 1996, pp. 387–411.

[13]Chung, Y. M., and Sung, H. J., "Comparative Study of Inflow Conditions for Spatially Evolving Simulation," *AIAA Journal*, Vol. 35, No. 2, 1997, pp. 269–274.

[14]Lund, T. S., Wu, X., and Squires, K. D., "Generation of Inflow a for Spatially-Developing Boundary Layer Simulations," *Journal of Computational Physics*, Vol. 140, No. 2, 1998, pp. 233–258.

[15]Li, N., Balaras, E., and Piomelli, U., "Inflow Conditions for Large Eddy Simulations of Mixing Layers," *Physics of Fluids*, Vol. 12, No. 4, 2000, pp. 935–938.

[16]Sagaut, P., *Large Eddy Simulation for Incompressible Flows—An Introduction*, 2nd ed., Springer-Verlag, Heidelberg, Germany, 2002.

[17]Druault, Ph., Lamballais, E., Delville, J., and Bonnet, J. P., "Development of Experiment/Simulation Interfaces for Hybrid Turbulent Results Analysis via the Use of DNS/LES," *Proceedings of the 1st International Symposium on Turbulence and Shear Flow Phenomena*, edited by S. Banerjee and J. K. Eaton, Begell House, New York, 1999, pp. 779–784.

[18]Lamballais, E., and Bonnet, J. P., "DNS/LES Data Processing and Its Relation with Experiments," von Kármán Inst. Course, April 2002, Paper 7.

[19]Maruyama, T., Rodi, W., Maruyama, Y., and Hiraoka, H., "LES Simulation of the Turbulent Boundary Layer Behind Roughness Elements Using an Artificially Generated Inflow," *Journal of Wind Engineering and Industrial Aerodynamics*, Vol. 83, 1999, pp. 381–392.

[20]Lumley, J., "The Structure of Inhomogeneous Turbulent Flows," *Atmospheric Turbulence and Radio Wave Propagation*, edited by A. M. Yaglon and V. I. Tatarski, Nauka, Moscow, 1967, pp. 166–178.

[21]Aubry, N., Holmes, P., Lumley, J., and Stone, E., "The Dynamics of Coherent Structures in the Wall Region of a Turbulent Boundary Layer," *Journal of Fluid Mechanics*, Vol. 192, 1988, pp. 115–173.

[22]Sirovich, L., "Turbulence and the Dynamics of Coherent Structures," *Quarterly of Applied Mathematics*, Vol. XLV, No. 3, 1987, pp. 561–590.

[23]Delville, J., Ukeiley, L., Cordier, L., Bonnet, J. P., and Glauser, M., "Examination of Large-Scale Structures in a Turbulent Plane Mixing Layer. Part 1. Proper Orthogonal Decomposition," *Journal of Fluid Mechanics*, Vol. 391, 1999, pp. 91–122.

[24]Druault, Ph., "Développement d'Interfaces Expérience/Simulation. Application à l'Ecoulement de Couche de Mélange Plane Turbulente," Ph.D. Dissertation, Univ. of Poitiers, France, Dec. 1999.

[25]Adrian, R. J., "On the Role of Conditional Averages in Turbulence Theory," *Turbulence in Liquids: Proceedings of the 4th Biennal Symposium on Turbulence in Liquids*, edited by G. Pateson and J. Zakin, Science Press, Princeton, NJ, 1977, pp. 322–332.

[26]Picard, C., and Delville, J., "Pressure Velocity Coupling in a Subsonic Round Jet," *Heat and Fluid Flow*, Vol. 21, 2000, pp. 359–364.

[27]Bonnet, J. P., Cole, D. R., Delville, J., Glauser, M. N., and Ukeiley, L. S., "Stochastic Estimation and Proper Orthogonal Decomposition: Complementary Techniques for Identifying Structures," *Experiments in Fluids*, Vol. 17, 1994, pp. 307–314.

[28]Faghani, D., "Etude des Structures Tourbillonnaires de la Zone Proche d'un Jet Plan: Approche non Stationnaire Multidimensionnelle," Ph.D. Dissertation, Inst. National Polytechnique de Toulouse, France, Nov. 1998.

[29]Ewing, D., and Citriniti, J. H., "Examination of a LSE/POD Complementary Technique Using Single and Multi-Time Information in the Axisymmetric Shear Layer," *IUTAM Symposium on Simulation and Identification of Organized Structures in Flows*, edited by J. N. Soresen, E. J. Hopfinger, and N. Aubry, Kluwer Academic, Dordrecht, The Netherlands, 1999, Chap. 9.

[30]Payne, F., "Generalized Gram-Charlier Method for Curve Fitting Statistical Data," *AIAA Journal*, Vol. 7, 1969, pp. 2045, 2046.

[31]Rempfer, D., "Investigation of Boundary Layer Transition via Galerkin Projection of Empirical Eigenfunctions," *Physics of Fluids*, Vol. 8, No. 1, 1995, pp. 175–188.

[32]Druault, P., and Delville, J., "Representation of the Spatial Correlation Tensor of the Velocity in Free Turbulent Flows," *Compte Rendu de l'Académie des Sciences, Série IIb*, Vol. 328, No. 2, 2000, pp. 135–141.

[33]Druault, P., Lamballais, E., Delville, J., and Bonnet, J. P., "Comparative Study of Inflow Conditions for Direct Numerical Simulations of a 2D Spatially Developing Plane Mixing Layer," *Proceedings of the 4th ECCOMAS Conference*, Vol. 1, Pt. 1, edited by K. D. Papailiou, D. Tsahalis, J. Péraux, C. Hirsch, and M. Pandolfi, Wiley, New York, 1998, pp. 34–39.

[34]Lumley, J. L., "Stochastic Tools in Turbulence," *Applied Mathematics and Mechanics*, Vol. 12, edited by F. N. Frenkiel and G. Temple, Academic Press, New York, 1970, Chap. 4.

[35]Coiffet, F., Delville, J., and Lamballais, E., "DNS/LES of a Turbulent Mixing Layer Using Instantaneous Experimental Data as Inflow Conditions," *Advances in Turbulence IX: Proceedings of the 9th European Turbulence Conference*, edited by I. P. Castro, P. E. Hancock, and T. G. Thomas, CIMNE, Barcelona, 2002.

[36]Lardeau, S., Lamballais, E., and Bonnet, J. P., "Direct Numerical Simulation of a Jet Controlled by Fluid Injection," *Journal of Turbulence*, Vol. 3, 2002, pp. 1–25.

[37]Lele, S. K., "Compact Finite Difference Schemes with Spectral-Like Resolution," *Journal of Computational Physics*, Vol. 103, 1992, pp. 16–42.

[38]Bonnet, J. P., Delville, J., Druault, Ph., Sagaut, P., and Grohens, R., "Linear Stochastic Estimation of LES Inflow Conditions," *Proceedings of First Air Force Office of Scientific Research International Conference on DNS and LES*, edited by C. Liu, Z. Liu, and L. Sakell, Greyden Press, Columbus, OH, 1997, pp. 341–348.

[39]Sagaut, P., Troff, B., Le, T. H., and Ta, P. L., "Large Eddy Simulation of Turbulent Flow Past a Backward Facing Step with a New Mixed Scale SGS Model," *Notes on Numerical Fluid Mechanics*, edited by M. Deville, S. Gavrilakis, and I. L. Rhyming, Vieweg Verlag, Braunschweig, Germany, 1996, pp. 271–278.

F. Grinstein
Guest Editor